A Novel Methodology to Assimilate Sub-Path Flows in Bi-Level OD Matrix Estimation Process

Krishna N. S. Behara, Ashish Bhaskar, and Edward Chung

***Abstract*— Traditional bi-level origin-destination (OD) matrix estimation process adjusts the matrix (at the upper level) based on the deviation between the observed and simulated traffic counts. The problem is mathematically under-determined, and the quality of the solution can be enhanced by restricting the upper level search space with information from other sources. This paper presents a methodology that assimilates sub-path flows in the upper level objective function. The contributions of the study are two-fold: first, it proposes the idea of "structural comparison of sub-path flows" to relax the requirement of "known" penetration rate of vehicles' trajectories; second, it proposes an innovative upper level formulation where the structural difference between the observed and assigned sub-path flows is integrated with the traditional deviations between the observed and assigned link flows. The sub-path flows can be estimated from advanced data sources such as Bluetooth MAC scanner. The proposed methodology is tested using simulation on a realistic network from Brisbane, Australia and results indicate its practical relevance for situations when the penetration rate of Bluetooth trajectories is generally unknown. The proposed method has a better ability to maintain structural consistency and showed considerable improvements in the quality of OD estimates as compared to the traditional traffic counts-based approach.**

***Index Terms*— OD matrix estimation, bi-level optimization, Bluetooth, sub-path flows, gradient descent, OD structure, Brisbane.**

I. Introduction

ORIGIN - DESTINATION (OD) matrix is a tabular representation of travel demand (flows) from each origin to every other destination on the transport network. It is a vital input for different levels of transport modelling- ranging from traditional strategic planning of transport infrastructure to advanced real-time operations and control of the network.

Ground truth of OD flows for large scale road network can't be directly measured and is generally unknown. Traditionally, road network is equipped with loop detectors and

Manuscript received September 9, 2019; revised March 18, 2020 and May 16, 2020; accepted May 21, 2020. The research was supported by scholarship from QUT (QUTPRA, HDR tuition fee waiver and Excellence Top up). The Associate Editor for this article was J. Blum. *(Corresponding author: Ashish Bhaskar.)*

Krishna N. S. Behara and Ashish Bhaskar are with the Science and Engineering Faculty, School of Civil and Environmental Engineering, Queensland University of Technology, Brisbane, QLD 4000, Australia (e-mail: ashish.bhaskar@qut.edu.au).

Edward Chung is with the Electrical Engineering Department, The Hong Kong Polytechnic University, Hong Kong, and also with the Science and Engineering Faculty, School of Civil and Environmental Engineering, Queensland University of Technology, Brisbane, QLD 4000, Australia.

Digital Object Identifier 10.1109/TITS.2020.2998475

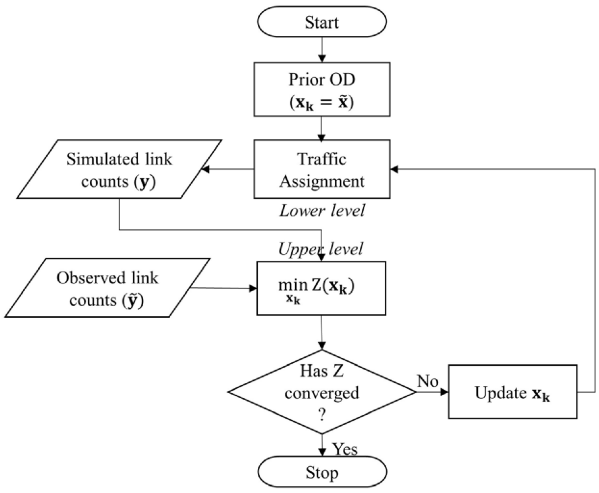

Fig. 1. Traffic counts-based bi-level OD estimation.

OD estimation process is modelled as a bi-level optimization problem [1], [2] where (*see* Fig.1): a) at upper level, the OD matrix ($\mathbf{x}$) is adjusted by minimising the gap between the observed ($\tilde{\mathbf{y}}$) and estimated ($\mathbf{y}$) traffic counts; and b) at lower level, traffic counts are estimated (simulated) by assigning traffic on the network using the adjusted OD matrix.

In Fig.1, the upper level formulation, is generally expressed in terms of observed ($\tilde{\mathbf{y}}$) and estimated ($\mathbf{y}$) link flows and assumes one of the following forms: Information minimization/entropy maximization [3]; maximum likelihood approach [4]; Bayesian inference methods [5], and generalized least squares (GLS) [1]. Equation 1 is the popular Spiess [6]'s upper-level formulation using matrix algebra.

$$\min_{\mathbf{x}} Z(\mathbf{x}) = \min_{\mathbf{x}} \frac{1}{2}\left(((\mathbf{y}-\tilde{\mathbf{y}}))^{\mathrm{T}}(\mathbf{y}-\tilde{\mathbf{y}})\right) \tag{1}$$

$$\text{subject to: } \mathbf{y} = \mathbf{P}\mathbf{x} \tag{1a}$$

The lower level of the bi-level framework runs traffic assignment ($\mathbf{P}$) that is either analytically derived [7] or simulation-based (say, from Aimsun [8], DYNASMART-P [9], TRANSIMS [10] etc.) or a combination of simulation and analytical formulation [11] or directly based on observations of travel speed/time [12] or turning proportions [13]. Alternatively, machine learning techniques have been explored to learn dynamic mapping (between OD and link flows) from observations of traffic data, thus independent of traditional assignment [14], [15]. They seem to be computational

efficient for demand estimation and prediction especially in real time. However, they cannot provide physical meanings of the assignment process as done by the existing analytical and simulation-based models [14].

Various techniques have been proposed to solve the upper-level formulation of the bi-level problem. They include gradient-based [6], gradient approximations [16]; and evolutionary algorithms (such as genetic algorithms, see [17]). Among these, gradient-based techniques are quite popular and different forms of the gradient-based techniques are applied in literature. This includes but not limited to coordinate descent method [18], projected gradient method [19], and the stochastic gradient method [20].

While most studies focused on different solution algorithms, OD estimation using traffic counts is still an under-determined problem. This is because a number of combinations of OD flows (or OD matrices of different structures) could exist to reproduce the same set of link flows, and thus the quality OD estimates cannot not be guaranteed if the objective function focusses only on the deviation of traffic counts [21]. This demands the need to maintain consistency in the structure of OD matrix (as per [22], [23] the trip distribution pattern between different OD pairs within an OD matrix defines the OD structure) during every iteration of bi-level estimation process [24]. To preserve the OD structure, most studies [1], [19], [25], [26] proposed to use target trip matrix ($\tilde{\mathbf{x}}$) in the objective function in order to confine the feasible region of OD estimates (refer Equation 2). The weight factors for objectives based on traffic counts and target OD matrix in Equation 2 are denoted by β_y and β_x, respectively.

$$\min_{x} Z(\mathbf{x}) = \min_{x} \frac{1}{2}\left(\left(\beta_y(\mathbf{y}-\tilde{\mathbf{y}})\right)^T(\mathbf{y}-\tilde{\mathbf{y}}) + \beta_x((\mathbf{x}-\tilde{\mathbf{x}}))^T(\mathbf{x}-\tilde{\mathbf{x}})\right) \tag{2}$$

$$\text{subject to: } \mathbf{y} = \mathbf{P}\mathbf{x} \tag{2a}$$

Researchers have also proposed constraints outside the objective function to maintain structural consistency. For instance, [24] proposed constraints on the columns of OD matrix using additional information from parking surveys, and [17] proposed constraints on the rows of OD matrix using the ratio of OD flows to origin flows. However, the prior knowledge (either in the form of target OD or trip production/attraction constraints) is based on outdated travel surveys and can lead to biased estimates [1].

With the availability of big traffic data, several researchers proposed to use travel speeds [27], travel times [28], turning proportions [29] and trajectory/partial path flow data [30], [31] into OD estimation problem. While some tried to infer OD matrices directly from the trajectory data such as taxi trajectories [15], [32], [33] or cellular probe [34];others tried to address the OD under-determinacy problem by introducing this information directly into the formulation where the deviations of observed and estimated path flows were minimized. Here, the penetration rate of observed path flows was either assumed to be known [30], [31], [35] or estimated [36], [37]. For instance, [31] assumed that penetration rates of Bluetooth counts is same as that of Bluetooth trajectories and used it to scale-up the vehicle trajectories in the objective function; [37] used simulator-based approach to estimate the scaling factor of trajectories that are inferred from call detail records. Thus, no technique has been proposed until now to use flows inferred from vehicle trajectories (we refer them as sub-path flows and are defined in the next paragraph) into the OD estimation formulation without prior knowledge of their penetration rates.

The following definitions regarding the sub-paths and sub-path flows are made in this study:

1. Sub-path (b): is defined as the portion of a complete traversed path. For instance, sub-path inferred by Bluetooth sensors is represented as a sequence of Bluetooth MAC scanner (BMS) detections.
2. Sub-path flows (s_b): are the flows passing through the sub-path (b). The vector representing sub-path flows from different sub-paths is represented using $\tilde{\mathbf{s}}$. For instance, the Bluetooth trajectories count over the sub-path can be used as the sub-path flows (refer 38] about method to estimate Bluetooth trajectories over the network).
3. Structure of sub-path flows: is defined as the arrangement of the sub-path flow values within the vector $\tilde{\mathbf{s}}$. More details about it are presented in Section III (*Method of comparison*).

A sub-path can also be considered as a sequence of links. If it constitutes only two detections at the extreme ends of a road segment, then sub-path flows refer to link flows. If the vehicle's trip is continuously monitored (as in GPS) from its origin until its destination, then sub-path represents a complete path. However, misdetections at a few sensor locations (as in case with Bluetooth scanners) could result in many such sub-paths for the same trip. Using flows from those sub-paths can lead to redundancy in the information as they relate to the same original trip. Thus, right selection of un-correlated sub-path flows is crucial in the OD estimation problem. However, sub-path flows capture trip distribution better than the point-based link flows, and any additional trip distribution information in the objective function tends to improve the quality of OD estimate.

The contributions of this study are two-fold. First, it proposes the idea of "structural comparison of sub-path flows" to relax the requirement of "known" penetration rate of vehicles' trajectories. To our knowledge, no study in the past has proposed such a method to deal with unknown penetration rates. Second, it develops a new upper level formulation by using the structure of sub-path flows as a penalty/scaling factor for the traditional traffic counts-based OD estimation. The formulation is novel and has not been considered in the literature.

The proposed approach is generic and as the proof of the concept, a synthetic network of Bluetooth-based sub-path flow information, and a gradient descent algorithm for OD estimation are considered in this paper. The methodology is thoroughly tested on a simulation model from Brisbane, Australia.

The remainder of the paper is structured as follows: Section II describes the notations of terms used in this study;

Section III discusses the proposed methodology; Section IV focusses on the experiments and results; Section V discusses the results of experiments; and finally the study concludes in Section VI with future study recommendations.

II. Notations of the Terms

In order to describe the formulations relevant to this paper, the following mathematical notations are used.

- The cardinality of a set is represented using |. |
- $\mathcal{A}$ denotes set of selected links of the study network; $\tilde{y}_a$ and y_a represent observed (say, from loop detectors) and simulated traffic counts/link flows on link $a \in \mathcal{A}$. $\tilde{\mathbf{y}} \in R_{\geq 0}^{|\mathcal{A}|}$ and $\mathbf{y} \in R_{\geq 0}^{|\mathcal{A}|}$ denote vectors of observed and simulated link flows, respectively
- $\mathcal{H}$ represents set of complete vehicle trajectories in a study network. $\mathcal{B}$ denotes set of sub-paths and $\mathcal{L}$ represent the total set of actual sub-trajectories (say, as sequence of BMS IDs) along $|\mathcal{B}|$ sub-paths. If the study performs analysis on only a random sample of sub-trajectories ($\tilde{\mathcal{L}}$), then we define $\eta = \left|\tilde{\mathcal{L}}\right| \Big/ |\mathcal{L}|$. Here, η_b is used to represent the penetration rate of observed vehicle trajectories on sub-path b. $\boldsymbol{\eta} \in R_{\geq 0}^{|\mathcal{B}|}$ is vector representing market penetration rates of observed trips on $|\mathcal{B}|$ sub-paths
- D denotes days of similar travel patterns. s_b^*, $\tilde{\mathbf{s}}_{b,d}$, $\tilde{\mathbf{s}}_b$ and s_b represent actual, observed (say, from Bluetooth) on d^{th} day ($d \in \mathbb{N}^{|D|}$), consolidated observations over $|D|$ days, and simulated sub-path flows on a sub-path $b \in B$, respectively. $\mathbf{s^*} \in R_{\geq 0}^{|\mathcal{B}|}$, $\tilde{\mathbf{s}}_\mathbf{d} \in R_{\geq 0}^{|\mathcal{B}|}$, $\tilde{\mathbf{s}} \in R_{\geq 0}^{|\mathcal{B}|}$ and $\mathbf{s} \in R_{\geq 0}^{|\mathcal{B}|}$ denote vectors of actual, observed (on d^{th} day), observed (consolidated over $|D|$ days), and simulated sub-path flows, respectively. $\boldsymbol{\mu}_{\mathbf{s^*}} \in R_{\geq 0}^{|\mathcal{B}|}$ is a vector with each cell value equal to mean of flow values in $\mathbf{s^*}$, and similarly $\boldsymbol{\mu}_{\tilde{\mathbf{s}}} \in R_{\geq 0}^{|\mathcal{B}|}$, $\boldsymbol{\mu}_{\mathbf{s}} \in R_{\geq 0}^{|\mathcal{B}|}$ correspond to $\tilde{\mathbf{s}}$ and $\mathbf{s}$, respectively
- W denotes set of OD pairs in the study network. x_w represents the number of estimated non-negative trips (by car) for OD pair $w \in W$, and similarly $\tilde{\mathbf{x}}_w$ and x_w^* are for prior and true OD flows. $\mathbf{x} \in R_{\geq 0}^{|W|}$, $\tilde{\mathbf{x}} \in R_{\geq 0}^{|W|}$, and $\mathbf{x^*} \in R_{\geq 0}^{|W|}$ denote estimated, prior, and true OD vectors, respectively. $\boldsymbol{\mu}_\mathbf{x} \in R_{\geq 0}^{|W|}$ is a vector with each cell value equal to mean of $\mathbf{x}$. Similarly, $\boldsymbol{\mu}_{\tilde{\mathbf{x}}} \in R_{\geq 0}^{|W|}$ and $\boldsymbol{\mu}_{\mathbf{x^*}} \in R_{\geq 0}^{|W|}$ correspond to $\tilde{\mathbf{x}}$ and $\mathbf{x^*}$, respectively.
- p_w^a is proportion of trips between w^{th} OD pair passing through link a. $\mathbf{P} \in R_{\geq 0}^{|\mathcal{A}|\times|W|}$ represents the link proportion matrix with p_w^a being the cell values.
- q_w^b is proportion of trips between w^{th} OD pair passing through sub-path b. $\mathbf{Q} \in R_{\geq 0}^{|\mathcal{B}|\times|W|}$ represents the sub-path proportion matrix with q_w^b being the cell values.

III. Proposed Methodology

The original objective function of OD estimation is based on the deviations of traffic counts (link flows). We know that link counts are only point-based measurements and are not meant to represent trip distribution very well. Matching both link flows and trip distribution (as two different objectives) could mitigate the OD under-determinacy problem to some extent. Direct observations of path flows help to account for the trip distribution. However, in situations where complete path flows cannot be observed, partial observations of path flows (we term them as sub-path flows in this paper) could possibly serve the purpose better than using only link flows. Thus, matching sub-path flows in addition to the link flows in the upper-level formulation should take care of both the objectives. However, in most cases, the market penetration rates of sub-path flows are generally unknown, and in such situations, we need an alternative measure of comparing sub-path flows. This is where the paper contributes by suggesting

a) *A method of comparison:* between observed (sample) and simulated sub-path flows.
b) *A way to integrate*: the above method of comparison into the existing upper level formulation of OD estimation problem.

Method of comparison: The method proposed to compare sub-path flows is through the concept of "structure". We assume that the structure of observed sample sub-path flows ($\tilde{\mathbf{s}}$) can be used as a proxy for the structure of actual sub-path flows ($\mathbf{s^*}$). Thus, expressing in terms of structural comparison between $\tilde{\mathbf{s}}$ (i.e. sample) and $\mathbf{s}$ should be equivalent to the structural comparison between "actual" sub-path flows and $\mathbf{s}$. We have used Pearson correlation coefficient (ρ) for the structural comparison of sub-path flows in our study. A higher correlation implies that both vectors (i.e.$\tilde{\mathbf{s}}$**ands**) are structurally closer to each other. This concept is borrowed from bio-medical analytics discipline where models with high dimensional data points are updated using similarity measures such as correlation coefficient [39].

Way to integrate: The structural comparison of sub-paths flows needs to be integrated into the upper-level formulation. One way is to consider as a weighted sum of two different objectives. However, we have noticed in our experiments that the deviation of traffic counts is dominating the objective function and there is no improvement in the OD structure despite giving high weightage to the structural comparison of sub-path flows. Therefore, we propose to model the sub path deviations (second objective) as a penalty/scaling factor to the traffic counts deviation (first objective). To achieve this, the formulation should be designed as a product of the two objectives.

The proposed methodology is illustrated in Fig.2. The new upper level formulation ($Z(\mathbf{x})$) includes two objectives: one based on traffic counts ($\tilde{\mathbf{y}}$ and $\mathbf{y}$) and other based on sub-path flows ($\tilde{\mathbf{s}}$ and $\mathbf{s}$).

Details into the development of the objective function formulation, method of gradient-based OD estimation, procedure to implement the proposed approach, and development of Bluetooth-based sub-path flows are presented in Section III.A, Section III.B, Section III.C, and Section III.D, respectively.

A. Proposed Objective Function Formulation

The new upper-level formulation can be expressed in terms of the deviation between the observed ($\tilde{\mathbf{y}}$) and estimated ($\mathbf{y}$) link flows and the structural comparison between observed ($\tilde{\mathbf{s}}$)

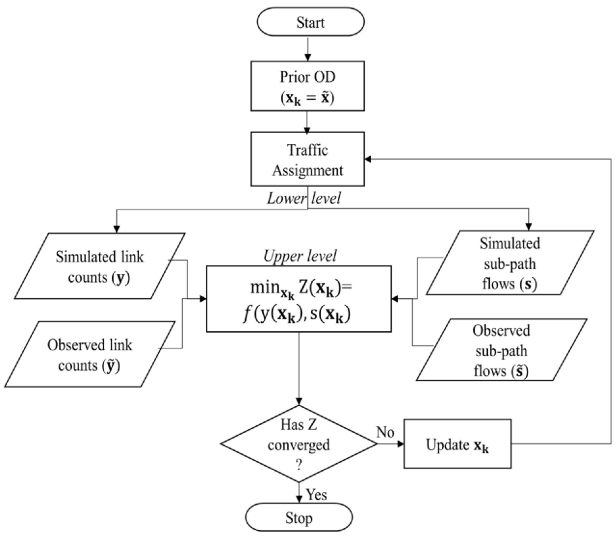

Fig. 2. Generic OD estimation algorithm based on the proposed approach.

and simulated ($\mathbf{s}$) sub-path flows as shown in Equation 3.

$$\min_{\mathrm{x}} Z(\mathbf{x}) = \min_{\mathrm{x}} \frac{1}{2}\left(\left(\mathrm{c}_1 + (\mathbf{y}-\tilde{\mathbf{y}})^{\mathrm{T}}(\mathbf{y}-\tilde{\mathbf{y}})\right)\right) \left((\mathrm{c}_2 + f(\mathbf{s},\tilde{\mathbf{s}}))^{\mathrm{T}}(\mathrm{c}_2 + f(\mathbf{s},\tilde{\mathbf{s}}))\right) \tag{3}$$

$$f(\mathbf{s},\tilde{\mathbf{s}}) = \frac{1-\rho(\mathbf{s},\tilde{\mathbf{s}})}{2} \tag{3a}$$

$$\text{such that } \mathbf{y} = \mathbf{P}\mathbf{x}; \quad \mathbf{s} = \mathbf{Q}\mathbf{x} \tag{3b}$$

$$\rho(\mathbf{s},\tilde{\mathbf{s}}) = \frac{(\tilde{\mathbf{s}}-\boldsymbol{\mu}_{\tilde{\mathbf{s}}})^{\mathrm{T}}(\mathbf{s}-\boldsymbol{\mu}_{\mathbf{s}})}{\sqrt{(\tilde{\mathbf{s}}-\boldsymbol{\mu}_{\tilde{\mathbf{s}}})^{\mathrm{T}}(\tilde{\mathbf{s}}-\boldsymbol{\mu}_{\tilde{\mathbf{s}}})}\sqrt{(\mathbf{s}-\boldsymbol{\mu}_{\mathbf{s}})^{\mathrm{T}}(\mathbf{s}-\boldsymbol{\mu}_{\mathbf{s}})}} \tag{3c}$$

The first objective is $\mathrm{c}_1 + (\mathbf{y}-\tilde{\mathbf{y}})^{\mathrm{T}}(\mathbf{y}-\tilde{\mathbf{y}})$ and the second objective is $\mathrm{c}_2 + \frac{1-\rho(\mathbf{s},\tilde{\mathbf{s}})}{2}$. Here, c_1 and c_2 are the stability constants. With non-zero c_1 ($\ll$1) if the deviation of traffic counts is equal to zero then the objective function should focus on minimising the second objective. The second objective considers any structural differences between the estimated/simulated and observed trip distribution from the perspective of sub-path flows. This acts as a scaling factor to the original traffic counts-based objective. The similarity measure ($\rho(\mathbf{s},\tilde{\mathbf{s}})$) is converted to a dissimilarity measure ($\frac{1-\rho(\mathbf{s},\tilde{\mathbf{s}})}{2}$) with the addition of a constant "c_2". This implies, when $\rho(\mathbf{s},\tilde{\mathbf{s}}) = 1$, $\mathrm{Z}(\mathbf{x})$ is multiplied by a factor of c_2^2 and for $\rho(\mathbf{s},\tilde{\mathbf{s}}) = -1$, $\mathrm{Z}(\mathbf{x})$ is scaled up $(\mathrm{c}_2{+}1)^2$ times.

What should be the value of c_2? Ideally, $\mathrm{c}_2 + \left(\frac{1-\rho(\mathbf{s},\tilde{\mathbf{s}})}{2}\right) \neq 0$

a) When structures of $\mathbf{s}$ and $\tilde{\mathbf{s}}$ are same then $\rho(\mathbf{s},\tilde{\mathbf{s}})$ is equal to 1 and $\left(\mathrm{c}_2 + \frac{1-\rho(\mathbf{s},\tilde{\mathbf{s}})}{2}\right) \Rightarrow \mathrm{c}_2$. Here, the objective function, $Z(\mathbf{x})$, is multiplied by a factor of c_2^2. Therefore, $\mathrm{c}_2 = 0$ should not be considered as it will make the objective function zero.
b) When structures of $\mathbf{s}$ and $\tilde{\mathbf{s}}$ are extremely opposite then $\rho(\mathbf{s},\tilde{\mathbf{s}})$ is equal to -1 and $\left(\mathrm{c}_2 + \frac{1-\rho(\mathbf{s},\tilde{\mathbf{s}})}{2}\right) \Rightarrow (\mathrm{c}_2{+}1)$. Here, the objective function, $Z(\mathbf{x})$ is multiplied by a factor of $(\mathrm{c}_2{+}1)^2$. Therefore, $\mathrm{c}_2 = -1$ should not be considered as it will make the objective function zero.

For the current study we consider $\mathrm{c}_2 = 1$. In this case,

a) When the structures of $\mathbf{s}$ and $\tilde{\mathbf{s}}$ are same then $Z(\mathbf{x})$ reduces to a traditional link counts deviation; that is, $\frac{1}{2}\left(\mathrm{c}_1 + (\mathbf{y}-\tilde{\mathbf{y}})^{\mathrm{T}}(\mathbf{y}-\tilde{\mathbf{y}})\right)$. This implies that simulated trip distribution matches the actual trip distribution, and simply minimizing traffic counts deviations should be sufficient to estimate OD.
b) When the structures of $\mathbf{s}$ and $\tilde{\mathbf{s}}$ are extremely opposite, the objective function multiplies $(2)^2$ times and becomes $2\left(\mathrm{c}_1 + (\mathbf{y}-\tilde{\mathbf{y}})^{\mathrm{T}}(\mathbf{y}-\tilde{\mathbf{y}})\right)$. This implies that deviation between traffic counts are amplified considering the extreme variations in the sub-path flows.

B. Gradient-Based Method for Optimization of the Objective Function

The gradient descent optimization method is used to iteratively update $\mathbf{x}$. The updating step is based on two major factors: search direction and step-size (λ):

a) The search direction is determined by the gradient of $Z(\mathbf{x})$. The step-size (λ) parameter determines the number of iterations required for the convergence. Lower values of λ ensure that the path of the gradient is smooth but computationally expensive. Higher values of λ can lead to higher values of the objective function, and the convergence could be affected.

Assuming $\mathbf{P}$ and $\mathbf{Q}$ are locally constant,[1] the functions involved in Equation 3 are differentiable with respect to $\mathbf{x}$ and its gradient is expressed as shown in Equation 4 and 4a.

$$\frac{\partial Z(\mathbf{x})}{\partial \mathbf{x}} = \frac{\partial\left(\frac{1}{2}\left(\mathrm{c}_1 + (\mathbf{y}-\tilde{\mathbf{y}})^{\mathrm{T}}(\mathbf{y}-\tilde{\mathbf{y}})\right)(\mathrm{c}_2 + f(\mathbf{s},\tilde{\mathbf{s}}))^{\mathrm{T}}(\mathrm{c}_2 + f(\mathbf{s},\tilde{\mathbf{s}}))\right)}{\partial \mathbf{x}} \tag{4}$$

$$= \left(\mathrm{c}_1 + (\mathbf{y}-\tilde{\mathbf{y}})^{\mathrm{T}}(\mathbf{y}-\tilde{\mathbf{y}})\right)(\mathrm{c}_2 + f(\mathbf{s},\tilde{\mathbf{s}}))\frac{\partial(f(\mathbf{s},\tilde{\mathbf{s}}))}{\partial \mathbf{x}} + (\mathrm{c}_2 + f(\mathbf{s},\tilde{\mathbf{s}}))^{\mathrm{T}}(\mathrm{c}_2 + f(\mathbf{s},\tilde{\mathbf{s}}))(\mathbf{y}-\tilde{\mathbf{y}})\mathbf{P}^{\mathrm{T}} \tag{4a}$$

using $\mathbf{y} = \mathbf{P}\mathbf{x}$
where

$$\frac{\partial(f(\mathbf{s},\tilde{\mathbf{s}}))}{\partial \mathbf{x}} = -\frac{1}{2}\frac{\partial(\rho(\mathbf{s},\tilde{\mathbf{s}}))}{\partial \mathbf{x}} \tag{4b}$$

Using the mapping relationship ($\mathbf{Q}$) between $\mathbf{s}$ and $\mathbf{x}$, Equation 3c can be simplified as shown in Equation 5.

$$\rho(\mathbf{Q}\mathbf{x},\tilde{\mathbf{s}}) = \frac{(\tilde{\mathbf{s}}-\boldsymbol{\mu}_{\tilde{\mathbf{s}}})^{\mathrm{T}}(\mathbf{Q}\mathbf{x}-\boldsymbol{\mu}_{\mathbf{Q}\mathbf{x}})}{\sqrt{(\tilde{\mathbf{s}}-\boldsymbol{\mu}_{\tilde{\mathbf{s}}})^{\mathrm{T}}(\tilde{\mathbf{s}}-\boldsymbol{\mu}_{\tilde{\mathbf{s}}})}\sqrt{(\mathbf{Q}\mathbf{x}-\boldsymbol{\mu}_{\mathbf{Q}\mathbf{x}})^{\mathrm{T}}(\mathbf{Q}\mathbf{x}-\boldsymbol{\mu}_{\mathbf{Q}\mathbf{x}})}} = \frac{\Gamma_1}{\sqrt{\Gamma_2}\sqrt{\Gamma_3}} \tag{5}$$

[1]The OD estimation presented in this paper is only for an hour OD that is assigned in the simulator using stochastic route choice. Traffic is assigned in Aimsun through a dynamic scenario and due to which the mapping relationships change dynamically during the hour simulation. However, the matrices **P/Q** are estimated using a back-calculation procedure based on one hour of aggregated link/sub-path flows that are resulted from Aimsun in every iteration. Thus **,** $\mathbf{P}$ and $\mathbf{Q}$ are only locally constant and change every time OD is updated.

where

$$\Gamma_1 = (\tilde{\mathbf{s}} - \boldsymbol{\mu}_{\tilde{\mathbf{s}}})^{\mathrm{T}} \left(\mathbf{Q}\mathbf{x} - \boldsymbol{\mu}_{\mathbf{Q}\mathbf{x}}\right) \tag{5a}$$

$$\Gamma_2 = (\tilde{\mathbf{s}} - \boldsymbol{\mu}_{\tilde{\mathbf{s}}})^{\mathrm{T}} (\tilde{\mathbf{s}} - \boldsymbol{\mu}_{\tilde{\mathbf{s}}}) \tag{5b}$$

$$\Gamma_3 = \left(\mathbf{Q}\mathbf{x} - \boldsymbol{\mu}_{\mathbf{Q}\mathbf{x}}\right)^{\mathrm{T}} \left(\mathbf{Q}\mathbf{x} - \boldsymbol{\mu}_{\mathbf{Q}\mathbf{x}}\right) \tag{5c}$$

Now, $\frac{\partial \rho(\mathbf{Q}\mathbf{x},\tilde{\mathbf{s}})}{\partial \mathbf{x}}$ can be expressed as shown in Equation 6.

$$\frac{\partial \rho\left(\mathbf{Q}\mathbf{x},\tilde{\mathbf{s}}\right)}{\partial \mathbf{x}} = \frac{\mathbf{Q}^{\mathbf{T}}\left((\tilde{\mathbf{s}} - \boldsymbol{\mu}_{\tilde{\mathbf{s}}}) - \frac{\Gamma_1}{\Gamma_3}\left(\mathbf{Q}\mathbf{x} - \boldsymbol{\mu}_{\mathbf{Q}\mathbf{x}}\right)\right)}{\sqrt{\Gamma}_2\sqrt{\Gamma}_3} \tag{6}$$

Thus, the differential objective function provides opportunities to consider standard gradient-based method to update the OD vector; that is, during any k$^{\text{th}}$ iteration $\mathbf{x_k}$ is updated to $\mathbf{x_{k+1}}$ using the search direction and optimal step-size as expressed in the Equation 7. Here, $Z(\mathbf{x})$ and $\mathbf{x}$ in $\frac{\partial Z(\mathbf{x})}{\partial \mathbf{x}}$ refer to the values corresponding to k$^{\text{th}}$ iteration. e is vector of 1s and of dimension same as $\mathbf{x}$ and Hadamard product "$\circ$" is used for element wise multiplication between λ_k and the gradient, and $\mathbf{x}_{\mathrm{k}}$ and $\left(e - \lambda_k \circ \frac{\partial Z(\mathbf{x})}{\partial \mathbf{x}}\right)$. Every iteration, the optimum λ_k is calculated as the solution to the objective function i.e. Equation 3.

$$\mathbf{x}_{\mathrm{k}+1}\mathbf{x}_{\mathrm{k}} \circ \left(e - \lambda_k \circ \frac{\partial Z\left(\mathbf{x}\right)}{\partial \mathbf{x}}\right) \tag{7}$$

$$\lambda_k \circ \frac{\partial Z\left(\mathbf{x}\right)}{\partial \mathbf{x}} < 1 \tag{7a}$$

C. Procedure to Implement the Proposed Methodology

To execute the framework illustrated in Fig. 2 under controlled environment, we need to run upper-level and lower optimizations one after another in an integrated manner. The step by step procedure for which is outlined below:

- Step-0: Obtain the observed sub-path flows ($\tilde{\mathbf{s}}$) and observed link flows ($\tilde{\mathbf{y}}$).
- Step-1: Set $k = 1$; $\mathbf{x_k} = \tilde{\mathbf{x}}$.
- Step-2: Load the study network in Aimsun next [40] with demand, $\mathbf{x_k}$ **,** and run traffic assignment (either stochastic route choice (SRC) assignment or dynamic user equilibrium). The outputs of the simulation are link flows ($\mathbf{y_k}$), sub-path flows ($\mathbf{s_k}$), link-proportion matrix ($\mathbf{P_k}$) and sub-path proportion-matrix ($\mathbf{Q_k}$).
- Step-3: Minimise the objective function, $Z(\mathbf{x})$ with respect to $\mathbf{x_k}$ (refer Equation 3).
- Step-4: Check for termination criterion, and if it is not met, set k: $= k+1$; update the demand ($\mathbf{x_k}$) for the next iteration (refer Equation 7), and go to Step 2. Else terminate the optimisation, and value of $\mathbf{x_k}$ is the final estimated OD vector.

The termination criterion can be either based on maximum relative change in the elements of estimated OD flows at successive iterations [7] or observed convergence for a fixed number of iterations [8].

For the current analysis, the codes for the optimisation are written in Matlab, and lower level traffic assignment is optimised using Aimsun next [40]. We have used the default parameter values for both demand scenarios and experiments

Fig. 3. Example to demonstrate Bluetooth sub-path.

in Aimsun. A Python script is written to integrate the optimisation model (in Matlab) with the traffic assignment (in Aimsun). However, Matlab is the primary platform that writes OD data into Aimsun OD format, runs the simulation, executes the Python script, and reads the simulation outputs for further optimisation process. This integration of Aimsun with Matlab is similar to the one presented in Antoniou *et al.* [21].

The aforementioned sections demonstrate that an additional objective based on sub-path flows can be incorporated into bi-level formulation. The next section discusses the development of sub-path flows from the network of BMS.

D. Bluetooth Sub-Path Flows

We assume that the road network is equipped with BMS [41]. For instance, in Brisbane, Australia we have over 1200 BMSs monitoring traffic on the Brisbane City Council (BCC) region[42]. The data from these network of BMSs can be integrated to define the trajectories of the Bluetooth vehicles [38]. The paths inferred from BMS detections are only sub-paths of actual paths traversed by vehicles. This is because, a) not all Bluetooth equipped vehicles are detected at the scanning zone; and b) the entire network is not fully equipped with the BMS, and the origin/destination BMS for the Bluetooth vehicle trajectory might not truly correspond to the true origin/destination zone for the network for which the OD is estimated.

For ease of understanding, refer to Fig. 3 that illustrates the difference between complete paths and a sub-path. Let's say the vehicle is detected from BMS1 to BMS5. The complete paths between the OD pairs A-C, A-D, B-C, and B-D share a common sub-path that can be represented as a sequence i.e. BMS1-BMS2-BMS3-BMS4-BMS5. Thus, it can be seen that it is not possible to infer the true trip ends (i.e. A/B and C/D) from the above sub-path.

Sometimes, a set of sub-paths can belong to the same trip due to missed detections. For instance, a missed detection at BMS3 in Fig. 3 could result in two sets of sub-paths, namely BMS1-BMS2, and BMS4-BMS5. In such cases the trips along those sub-paths can lead to redundancy in the information as they relate to the same original trip. Thus, right selection of un-correlated sub-paths is crucial in the OD estimation problem.

The penetration rate of Bluetooth-based counts at a specific level can range from 10%-30% [31]. However, the penetration rate for the observed path flows from BMS can be much lower say, around 5% ([43] reported 4.4% average detection rate for 12 OD pairs at an interchange level) and can vary over different paths. We address this issue of low sample rates

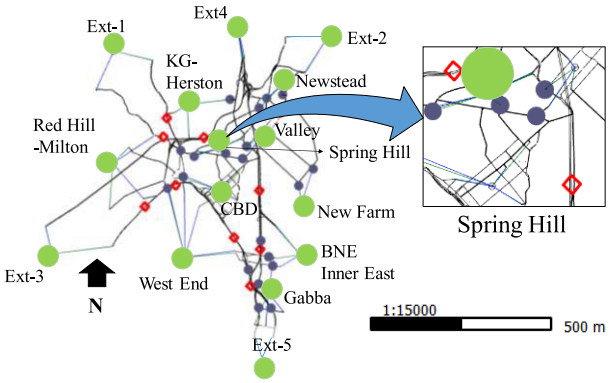

Fig. 4. Study site with Bluetooth scanners (solid blue circles), loop detectors (red rectangles) and zonal centroids (solid green circles).

as follows: We propose to generate a sub-path flow vector by combining sub-path flows observed from several days of similar travel patterns. For instance, the observed sub-path flows from $|D|$ regular working Mondays can be used to develop a consolidated vector of observed sub-path flows for a typical working Monday. Thus, $\tilde{\mathbf{s}}_b$ can be considered as a consolidation of several observations of Bluetooth flows on sub-path b as shown in Equation 8.

$$\tilde{\mathbf{s}}_b = \sum_{d=1}^{d=|D|} \tilde{\mathbf{s}}_{b,d} \tag{8}$$

The consolidated vector $\tilde{\mathbf{s}}$ can then be expressed as shown in Equation 9

$$\tilde{\mathbf{s}} = \sum_{d=1}^{d=|D|} \tilde{\mathbf{s}}_{\mathbf{d}} \tag{9}$$

IV. Experiments and Results

A. Study Network

To test the proposed methodology, the study network should have the following properties:

1. It should be realistic and representative of the existing infrastructure;
2. It should have enough route choice options;
3. It should have a combination of at least two different types of road hierarchy i.e. motorway and arterial;
4. OD pairs should have enough overlap between the paths;
5. It should have enough Bluetooth connectivity; that is, the sub paths should be along the major routes; and
6. Loop detectors to be located on important corridors.

The study network meeting the above-mentioned criteria is presented in Fig. 4. It represents the core of the Brisbane city network imported into Aimsun next from open street map [44]. The network comprises of 15 centroids (zones), 24 loop detectors (red squares in Fig. 4), and 20 Bluetooth scanners (blue circles in Fig. 4) and 5 external zones. The loop detectors and BMS are placed on the major roadways such as Pacific Motorway, Clem Jones Tunnel, Coronation Drive, Inner City Bypass, and Kelvin Grove Road.

The OD matrix is designed at a zonal level equivalent to Statistical Area 2 (SA2) ()[45] and is 15 x 15 in size. Internal trips are excluded in the analysis. Since, the number of OD pairs is greater than 200 it is a high dimensional OD matrix [46]. The 15 zonal centroids shown are:

- West End;
- Gabba;
- Brisbane (BNE) Inner East;
- New Farm;
- Fortitude Valley;
- Spring Hill;
- Central Business District (CBD);
- Newstead;
- Kelvin Grove(KG)–Herston;
- Red Hill–Milton; and
- Five external zonal centroids; that is, Ext-1, Ext-2, Ext-3, Ext-4, and Ext-5, respectively.

The traffic from each zone is loaded into to the network through several connectors. The zones, namely Ext-1, Ext-2, Ext-3, Ext-5 and New Farm have 2 connectors each; Ext-4, Kelvin Grove, Newstead and BNE Inner East have 3 each; West End, Red Hill-Milton, Valley, and Gabba have 4 each; and Brisbane CBD has 5 connectors, respectively. The number of paths per OD pair are chosen to be greater than one, and the paths connecting different OD pairs have enough overlap.

Each zone/centroid is connected by at least one BMS so that complete path can be identified as a sequence of BMS IDs between any OD pair. Although complete trajectories are available in the simulation, the analysis in this study is performed using Bluetooth sub-paths only. Refer Section IV.B for more details.

B. Design of Experiments

For the current analysis we aim to estimate typical OD for the network, given data from several days. For instance, we are interested in typical OD during morning peak hours of regular Monday using loop detector and BMS data from several regular Mondays. To generate synthetic data for such application we do the following:

a) Define number of similar OD matrices representing normal day-to-day travel demand variability. The average of these OD represents the typical OD and is the ground truth for the study. The details are presented in Section IV.B.1.

b) Simulate the traffic with an OD and export the loop and Bluetooth data. Repeat this process over all the defined ODs. This provides database for individual day loop counts and Bluetooth-based sub-path flows (refer Section IV.B.3.

1) Defining Similar OD Matrices: For the study network, we develop a database of OD matrices that are structurally similar. Here, we define a typical OD matrix $\mathbf{x}^*$ (one-hour demand equal to 6736 trips) and generate additional four similar OD matrices by randomly perturbing $\mathbf{x}^*$ with a standard deviation of 5%. The OD matrices are denoted by $\mathbf{x}_\mathbf{i}^*$ where $\mathbf{x}_\mathbf{1}^* = \mathbf{x}^*$ and $\mathbf{x}_\mathbf{i}^* = \text{rand}\,(\mathbf{x}^*, 5\%)\ \forall 2 \leq i \leq 5$ such that $x_{w,i}^* > 0$.

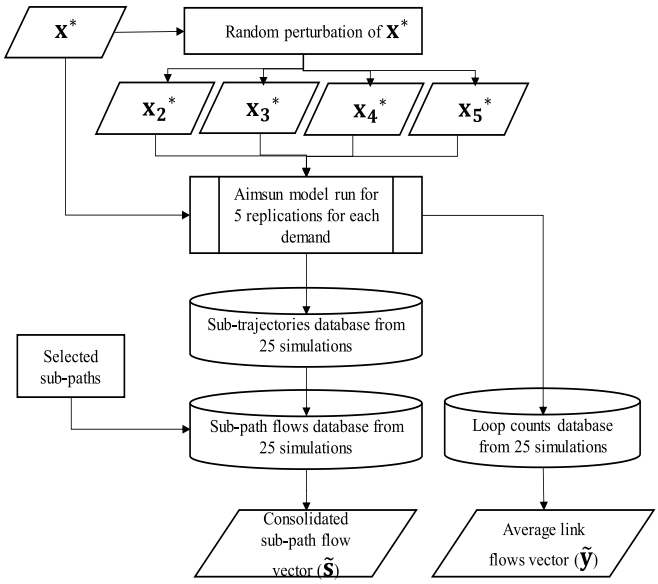

Fig. 5. Method to generate synthetic data ($\tilde{\boldsymbol{y}}$ and $\tilde{\boldsymbol{s}}$).

2) Traffic Simulation: For the current analysis, an hour (7:30 AM- 8:30 AM) of simulation is performed using Aimsun micro- which is a stochastic simulation at the microscopic level. The assignment model considered is stochastic route choice. The demand for each simulation is defined as per Section IV.B.1 resulting in five different scenarios for a typical OD. For each scenario five replications are simulated. Each replication has its own random seed, resulting in a simulation with different random selection of the stochastic parameters.

3) Synthetic Traffic Database (Loops and BMS): The traffic database consists of loops and Bluetooth records from a total of 25 simulation runs (5 similar demand patterns and 5 replications for each demand). Refer Fig. 5 that explains the process of generating $\tilde{\mathbf{s}}$ and $\tilde{\mathbf{y}}$.

The network has 24 loop detectors (see Fig. 4). Total vehicle counts at each detector location during each simulation run is obtained. Finally, traffic count at each detector location is defined by first considering average of the counts at the location from 25 simulations.

The network has 20 BMSs (see Fig. 4) that detects Bluetooth equipped vehicles. Interested readers can refer to the traffic and communication simulation model for simulating BMS dataset using Aimsun [41]. In this study, the sub-paths are pre-selected before conducting the analysis. The number of common sub-paths in all 25 simulation runs is identified to be $|\mathcal{B}| = 113$. For the analysis we have considered four different cases with Bluetooth penetration rates (see Section IV.B.4. Bluetooth sub-path trajectories are estimated independently for each case.

The process of generating $\tilde{\mathbf{y}}$ and $\tilde{\mathbf{s}}$ illustrated in Fig. 5 is briefly explained as follows:

- First, initiate $\tilde{\mathbf{y}}_{\mathbf{i,r}}$ and $\tilde{\mathbf{s}}_{\mathbf{i,r}}$ of dimensions $|\mathcal{A}| \times 1 = 24 \times 1$ and $|\mathcal{B}|\,\mathrm{x}1 = 113 \times 1$, respectively for i^{th} OD matrix ($\mathbf{x_i^*}$) and r^{th} replication with zero flow values.
- Second, simulated traffic counts from $|\mathcal{A}| = 24$ loops are denoted by $\tilde{\mathbf{y}}_{\mathbf{i,r}}$. The database of vehicle trajectories are stored as a complete sequence of BMS in $\mathcal{H}_{i,r}$. The first and last BMSs of each complete trajectory sequence are directly linked to the actual origin and destination zones of the simulated trip.
- Third, convert $\mathcal{H}_{i,r}$ to sub-trajectories ($L_{i,r}$) by de-selecting a few scanner IDs from the beginning and ending of the complete trajectory sequence (this is done because the actual Bluetooth trajectories do not always represent true trip ends) and due to the deselection process $|\mathcal{L}_{i,r}|$ is less than $|\mathcal{H}_{i,r}|$. For instance, $|\mathcal{H}_{1,1}| = 5,273$ and $|\mathcal{L}_{1,1}| = 3,875$ in our study.
- Fourth, identify η percent of sub-trajectories ($\tilde{\mathcal{L}}_{i,r}$) from the set $L_{i,r}$. For instance, $|\tilde{\mathcal{L}}_{1,1}| = 97$ for $\eta\% = 2.5\%$ of 3,875 of total sub-trajectories.
- Fifth, count the number of sub-trajectories (from $\tilde{\mathcal{L}}_{i,r}$) passing through each sub-path in $\mathcal{B}$ and add it to $\tilde{\mathbf{s}}_{\mathbf{i,r}}$. Note that $\eta\%$ random selection in the previous step might not account all sub-paths, and in such cases, some of the sub-paths can contain zero flow values in $\tilde{\mathbf{s}}_{\mathbf{i,r}}$. For instance, $|\tilde{\mathcal{L}}_{1,1}| = 97$ sub-trajectories (for $\eta\% = 2.5\%$) resulted in only 43 out of $|\mathcal{B}| = 113$ sub-paths, which means the flows for the rest are zeros. Similarly, 61 for 5%, 76 for 7.5%, and 82 for 10%, respectively.
- Repeat steps from first to fifth for all 25 simulations (i.e. $i = 1$ to 5 and $r = 1$ to 5). The average traffic counts observations are obtained as $\tilde{\mathbf{y}} = \frac{\sum_{i=1}^{5}\sum_{r=1}^{5}\tilde{\mathbf{y}}_{\mathbf{i,r}}}{\mathbf{25}}$ and the final consolidated vector of sub-path flows is obtained as $\tilde{\mathbf{s}} = \sum_{i=1}^{5}\sum_{r=1}^{5}\tilde{\mathbf{s}}_{\mathbf{i,r}}$.

TABLE I
STRUCTURAL SKEWNESS COMPARISON

$\eta\%$	$\left(\sum_{i=1}^{5}\sum_{r=1}^{5}\rho(\tilde{\mathbf{s}}_{i,r}, \mathbf{s}^*)\right)\Big/_{25}$	$\rho(\tilde{\mathbf{s}}, \mathbf{s}^*)$
2.5%	0.8033	0.9866
5.0%	0.8904	0.9961
7.5%	0.9212	0.9951
10.0%	0.9413	0.9973

The structural skewness of consolidated sub-path flows ($\tilde{\mathbf{s}}$) in comparison with average skewness for different $\eta\%$ is shown in Table I.

It can be seen in Table I that $\rho(\tilde{\mathbf{s}}, \mathbf{s^*})$ (i.e. 3rd column) is better than the average skewness (i.e. 2nd column). This implies that consolidation of sample sub-path flows ($\tilde{\mathbf{s}}_{\mathbf{i,r}}$) over several similar days improves the quality of $\tilde{\mathbf{s}}$.

4) Experiment Cases: To evaluate the impact of the Bluetooth penetration rate we consider different scenarios as follows:

a) *Traditional case:* $Z(\mathbf{x})$ is expressed only in terms of traffic counts deviations (Equation 1). No Bluetooth-based sub-path trajectories are considered.
b) *Case-1:* Here, $\tilde{\mathbf{s}}$ is generated using $\eta\% = 2.5\%$ and $Z(\mathbf{x})$ is expressed using Equation 3.
c) *Case -2:* Here, $\tilde{\mathbf{s}}$ is generated using $\eta\% = 5\%$ and $Z(\mathbf{x})$ is expressed using Equation 3.
d) *Case -3:* Here, $\tilde{\mathbf{s}}$ is generated using $\eta\% = 7.5\%$ and $Z(\mathbf{x})$ is expressed using Equation 3.

TABLE II
COMPARISON OF $\tilde{\mathbf{x}}_c$ WITH $\mathbf{x}^*$

Prior ODs ($\tilde{\mathbf{x}}_c$)	RMSN($\tilde{\mathbf{x}}_c, \mathbf{x}^*$)	$\rho(\tilde{\mathbf{x}}_c, \mathbf{x}^*)$
$\tilde{\mathbf{x}}_1$	0.47	0.8142
$\tilde{\mathbf{x}}_2$	0.57	0.6704
$\tilde{\mathbf{x}}_3$	0.61	0.5727

e) *Case -4:* Here, $\tilde{\mathbf{s}}$ is generated using $\eta\% = 10\%$ and $Z(\mathbf{x})$ is expressed using Equation 3.

C. Performance Evaluation

To check the efficiency of the proposed methodology, the final estimated OD ($\mathbf{x}$), individually for different cases, is compared with ground truth OD ($\mathbf{x^*}$) using following two indicators:

a) RMSN ($\mathbf{x}$,$\mathbf{x}^*$) (Equation 10): It is a standard measure to compare estimated OD flows (x_w) with that of ground truth (x_w^*). In the Equation 10, $|W|$ is the size of the OD vector.

b) $\rho(\mathbf{x},\mathbf{x^*})$ (Equation 11): This measure is more robust [22], 47] and is used to compare only the structural deviation between the estimated OD matrix ($\mathbf{x}$) and ground truth OD vector ($\mathbf{x^*}$). Notations of terms used in Equation 11 are explained in Section II.

$$\text{RMSN}\left(\mathbf{x},\mathbf{x^*}\right) = \frac{\sqrt{|W|\sum_{\text{w}\in\text{W}}\left(x_w - x_w^*\right)^2}}{\sum_{\text{w}\in\text{W}} x_w^*} \tag{10}$$

$$\rho\mathbf{x},\mathbf{x}^* = \frac{(\mathbf{x}-\boldsymbol{\mu}_{\mathbf{x}})^{\text{T}}(\mathbf{x}^*-\boldsymbol{\mu}_{\mathbf{x}^*})}{\sqrt{(\mathbf{x}-\boldsymbol{\mu}_{\mathbf{x}})^{\text{T}}(\mathbf{x}-\boldsymbol{\mu}_{\mathbf{x}})}\sqrt{(\mathbf{x}^*-\boldsymbol{\mu}_{\mathbf{x}^*})^{\text{T}}(\mathbf{x}^*-\boldsymbol{\mu}_{\mathbf{x}^*})}} \tag{11}$$

D. A Priori OD Matrix for Optimization

To test the proposed methodology with respect to the consideration of *a priori* OD matrix for optimization, we perform the analysis independently on three different *a priori* OD matrices ($\tilde{\mathbf{x}}_1$,$\tilde{x}_2$, and $\tilde{\mathbf{x}}_3$ in the descending order of OD quality). Table II presents the quality of *a priori* OD matrix ($\tilde{\mathbf{x}}_c$) with respect to the ground-truth ($\mathbf{x^*}$).

E. Results

In this section, we discuss the quality of the OD estimates ($\mathbf{x}$) resulted from different cases and consideration of different *a priori* OD matrices.

1) Quality Assessment of OD Estimates Using RMSN: The Fig. 6 summarizes the results using RMSN as the performance indicator. Here, different link graph corresponds to different *a priori*-OD matrix. The x-axis represents different cases.

The results indicate a gradual improvement in the quality of $\mathbf{x}$ as measured through RMSN. For instance, the set of experiments initiated with $\tilde{\mathbf{x}}_1$ improved from RMSN ($\tilde{\mathbf{x}}_1$,$\mathbf{x^*}$) = 0.47 to RMSN ($\mathbf{x}$,$\mathbf{x^*}$) = 0.38 (for $\eta\%$=10%). Similarly, the results for the experiments initiated with $\tilde{\mathbf{x}}_2$, and $\tilde{\mathbf{x}}_3$ have also demonstrated significant improvements.

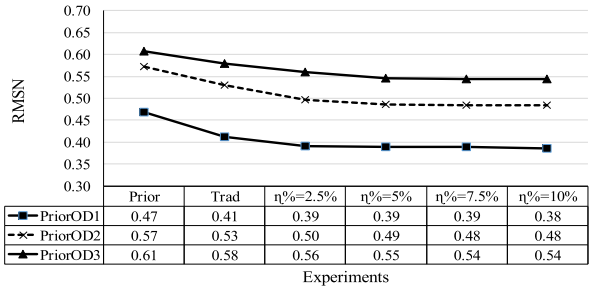

Fig. 6. RMSN ($\tilde{\boldsymbol{x}}_c, \boldsymbol{x}^*$) Vs $RMSN\left(\boldsymbol{x}, \boldsymbol{x}^*\right)$ for all experiments.

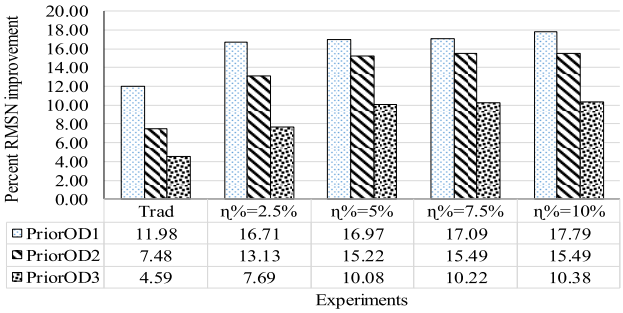

Fig. 7. % Improvements in $RMSN\left(\boldsymbol{x}, \boldsymbol{x}^*\right)$ with respect to RMSN ($\tilde{\boldsymbol{x}}_c, \boldsymbol{x}^*$).

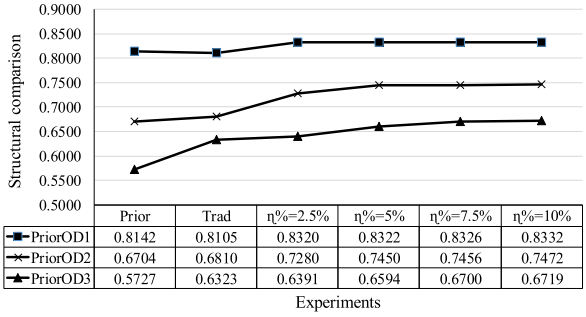

Fig. 8. ρ ($\tilde{\boldsymbol{x}}_c, \boldsymbol{x}^*$) Vs $\rho\left(\boldsymbol{x}, \boldsymbol{x}^*\right)$ for all experiments.

The percent improvements in RMSN ($\mathbf{x}$,$\mathbf{x}^*$) are illustrated in Fig. 7. The percent improvement is calculated with respect to $\tilde{\mathbf{x}}_c$, and we can observe greater improvements in all Bluetooth-based cases as against the traditional case. For example, at $\eta\%$=2.5%, there is 16.71% improvement (from RMSN ($\tilde{\mathbf{x}}_1$,$\mathbf{x}^*$) = 0.47 to RMSN ($\mathbf{x}$,$\mathbf{x}^*$) = 0.39. Within the Bluetooth based cases, there is only a slight improvement in the RMSN.

2) Quality Assessment of OD Estimates Using ρ: The ρ ($\mathbf{x}$,$\mathbf{x}^*$) results as shown in Fig. 8 demonstrate that there is structural improvement in the OD estimates as $\eta\%$ increases from 2.5% to 10%. Fig. 8 also highlights that the traditional traffic counts-based approach could not bring any significant structural improvements in the OD estimates unless additional information from Bluetooth sub-path flows is introduced.

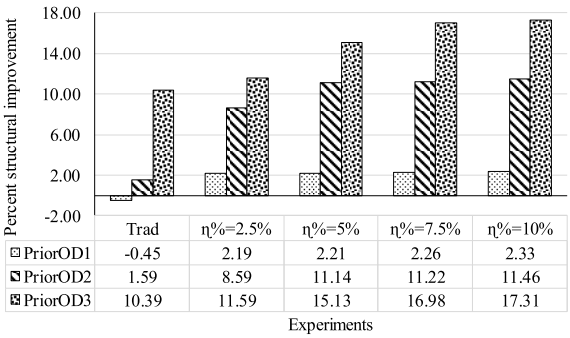

	Trad	η%=2.5%	η%=5%	η%=7.5%	η%=10%
PriorOD1	-0.45	2.19	2.21	2.26	2.33
PriorOD2	1.59	8.59	11.14	11.22	11.46
PriorOD3	10.39	11.59	15.13	16.98	17.31

Fig. 9. % Improvements in $\rho\left(\boldsymbol{x}, \boldsymbol{x}^*\right)$ with respect to $\rho(\tilde{\boldsymbol{x}}_C, \boldsymbol{x}^*)$.

TABLE III
STATISTICAL DIFFERENCE BETWEEN TRADITIONAL AND REST OF THE CASES

	$\text{RMSN}(\mathbf{x}, \mathbf{x}^*)$		$\rho(\mathbf{x}, \mathbf{x}^*)$	
	t-value	p-value	t-value	p-value
Trad. vs Case-1	7.000	0.020	-2.137	0.166
Trad. vs Case-2	5.196	0.035	-2.829	0.106
Trad. vs Case-3	4.158	0.053	-3.341	0.079
Trad. vs Case-4	6.928	0.020	-3.383	0.077

The percentage structural improvement in $\rho\,(\mathbf{x},\mathbf{x}^*)$ for the traditional method is negative for $\tilde{\mathbf{x}}_1$ based experiment (Fig. 9). This implies a structural degradation. The simulation runs based on $\tilde{\mathbf{x}}_2$ has also showed only little improvement while there is some improvement for $\tilde{\mathbf{x}}_3$. This shows that traffic counts-based OD estimation does not necessarily improve the structure of OD because the deviations of traffic counts used in the objective function do not capture any sort of OD structural information.

Another factor that could possibly control the results may be attributed to the selection of gradient descent algorithm. The current study focuses on the development of a new upper-level formulation, improving upon the solution algorithm is beyond the scope of this paper. Nonetheless, it can be seen that rates of improvement for sub-path flows-based cases are better than that of traditional method because they provide additional information related to trip distribution. While, the percent improvement in $\rho\ (\mathbf{x},\mathbf{x}^*)$ is higher for sub-path flows-based cases (i.e. case-1 to case-4), there is no significant difference in the improvements among them. This, is because the consolidated (for 25 simulations) penetration rates of $\eta\%$ =2.5%, 5%, 7.5% and 10% are2.5%∗25 = 62.5%, 5%∗25 = 125%, 7.5%∗187.5, and 10%∗2.5=250%, respectively, and are rather sufficient to bring the necessary improvement in the OD quality.

3) Statistical Assessment of the Results: The difference between the results obtained from traditional method and those from the cases with Bluetooth penetration rates are statistically compared at $\alpha = 10\%$ level of significance using paired t-test and are shown in the Table III. Although, the improvements in the absolute values of both RMSN (Fig. 6 and Fig. 7) and ρ (Fig. 8 and Fig. 9) seem to be marginal, Table II demonstrates that that the absolute t-values are greater than the critical value (i.e. +/-2.353 for 3 degrees of freedom) at 90% confidence level in all cases for RMSN and in all but case-1 for ρ. Except for ρ comparison in case-1, the results from traditional and proposed method are statistically different.

V. DISCUSSION

The goodness of fit measurements namely, RMSN $(\mathbf{x},\mathbf{x}^*)$ and $\rho\,(\mathbf{x},\mathbf{x}^*)$ showed significant improvement with respect to both *a priori* OD and traditional method using Bluetooth sub-path flows. We can see that the results for $\eta\% > 2.5\%$ (i.e. case-2 to case-4) are slightly better than $\eta\%$=2.5% (case-1).

The traditional method did not show any significant structural enhancements (Fig. 8 and Fig. 9) although the RMSN $(\mathbf{x},\mathbf{x}^*)$ measure is improved (refer to $\tilde{\mathbf{x}}_1$ and $\tilde{\mathbf{x}}_2$ cases in Fig. 6 and Fig. 7). In fact, RMSN $(\mathbf{x_1},\mathbf{x}^*)$ is improved but $\rho\,(\mathbf{x_1},\mathbf{x}^*)$ degraded due to the problem of under-determinacy for the traditional case. This showed that preserving the OD structure using additional path-based information from Bluetooth short trips (which we referred as sub-path flows in this paper) helped to direct OD convergence towards a better solution estimate instead of 'getting stuck' in the local optima.

There is hardly any difference in the computational cost required to evaluate traditional and proposed objective functions. For $\tilde{\mathbf{x}}_1$ scenario, the computational time (tested on a Dell computer with Intel(R) Core(TM) i5-3230 CPU, 4GB RAM, 2.60GHz) required for the traditional method is nearly 3.86 minutes and for the sub-path flows-based experiments it is around 3.78 minutes (average of all 4 cases).

The experiments are tested in a controlled environment due to the unavailability of the ground truth (i.e. true OD). Nevertheless, the study demonstrated the performance of proposed methodology for different prior OD matrices and lower sample of random Bluetooth observations. The Brisbane City Council (BCC) and the Department of Transport Main Roads (TMR) have been recording the Bluetooth observations on a continuous basis, and it is possible to have the database of traffic observations from several days representing similar travel patterns [48]. Thus, the proposed methodology is ready for practical implementation on real world networks with trajectories and loop counts database.

VI. CONCLUSION

One of the major limitations of traffic counts-based OD estimation is the problem of under-determinacy, and due to which the quality of OD estimates cannot always be guaranteed. With the advancements in technology, many emerging data sources such as Bluetooth provides additional travel related information including vehicle trajectories. However, they are only partial observations of complete trips with random and unknown penetration rates. Studies in the past have developed objective functions based on partial path (referred as sub-path in this study) information but with an assumption that their penetration rate is known.

To this end, the study contributes in two ways: first, it proposes the idea of "structural comparison of sub-path flows" to relax the requirement of "known" penetration rate of vehicles' trajectories; second, it proposes an innovative

way to incorporate the sub-path flow information in the upper level objective function of the traditional bi-level optimization problem of OD estimation. Here, the structural difference between the observed and estimated sub-path flows is modelled as the correlation coefficient and integrated with the traditional objective to minimize the deviation between the observed and estimated link flows. The proposed objective function is the product of two functions, one measuring the fit in the link flows, the other one measuring correlation in sub-path flows. In this formulation when the structure of the observed and estimated sub-path flows has: a) perfect positive correlation ($= +1$), then the formulation reduces to the traditional minimization of the link flows; and b) imperfect negative correlation ($=-1$), then the formulation amplifies the deviations of the link flows.

The proposed sub-paths flows-based approach maintains structural consistency in the OD matrix estimates and is better than traditional traffic counts-based technique. This is because the structure of Bluetooth sub-path flows, which is independent of the penetration rates, provides an additional higher-dimensional information about trip distribution as against point-based observations of link flows. The proposed methodology, tested through several experiments, has demonstrated its practical relevance for situations when the penetration rate of Bluetooth trajectories is low.

While the present study demonstrated results better than the traditional approach, the study can be extended in the following research directions. First, this study is a proof of concept where we focus on the formulation of the upper level objective function and have applied traditional gradient descent approach for optimization. This provides conservative results. Also, the step size is crucial in gradient descent algorithm and needs to be adjusted for different OD flow values. The consideration of advanced stochastic algorithms such as stochastic perturbation and simultaneous approximation (SPSA) and Genetic Algorithms should further improve the results. Second, more experiments shall be conducted in future to investigate right selection of sub-paths, the percentage of OD demand they are able to intercept (similar to [49], [50] where the results showed improvement for both intercepted and non-intercepted OD), and the sensitivity of the selected sub-path flows on OD estimation. Third, the study uses average traffic counts for D days. Averaging counts may be acceptable for demand realizations that are relatively close to each other. However, in the real world, since the underlying demand is unknown, there is little chance to verify this assumption. This is particularly so if major incidents were active during the data collection. As a part of the future study, we would like to test our approach for such situations. Finally, the current study is based on a synthetic network, but the real network is challenged by errors, unobserved stochasticity, unknown true demand etc. Thus, we would like to test our methodology on a real case study network for the future study as well.

Although, the study demonstrated using Bluetooth sub-path flows, the proposed approach is generic in nature and the formulation holds good for path (partial/complete) flows observed from any other emerging data sources such as WiFi, GPS, mobile phone etc.

ACKNOWLEDGMENT

The conclusions of this article reflect understandings of the authors, who are responsible for the accuracy of the research findings.

REFERENCES

[1] E. Cascetta, "Estimation of trip matrices from traffic counts and survey data: A generalized least squares estimator," *Transp. Res. B, Methodol.*, vol. 18, nos. 4–5, pp. 289–299, Aug. 1984.

[2] G. Cantelmo, E. Cipriani, A. Gemma, and M. Nigro, "An adaptive bi-level gradient procedure for the estimation of dynamic traffic demand," *IEEE Trans. Intell. Transp. Syst.*, vol. 15, no. 3, pp. 1348–1361, Jun. 2014.

[3] H. J. Van Zuylen and L. G. Willumsen, "The most likely trip matrix estimated from traffic counts," *Transp. Res. B, Methodol.*, vol. 14, no. 3, pp. 281–293, Sep. 1980.

[4] H. Spiess, "A maximum likelihood model for estimating origin-destination matrices," *Transp. Res. B, Methodol.*, vol. 21, no. 5, pp. 395–412, Oct. 1987.

[5] M. Maher, "Inferences on trip matrices from observations on link volumes: A Bayesian statistical approach," *Transp. Res. B, Methodol.*, vol. 17, no. 6, pp. 435–447, 1983.

[6] H. Spiess, "A gradient approach for the OD matrix adjustment problem," Centre Res. Transp., Univ. Montreal, Montreal, QC, Canada, Publication No. 693.

[7] M. J. Maher, X. Zhang, and D. V. Vliet, "A bi-level programming approach for trip matrix estimation and traffic control problems with stochastic user equilibrium link flows," *Transp. Res. B, Methodol.*, vol. 35, no. 1, pp. 23–40, Jan. 2001.

[8] M. Bullejos, J. Barceló Bugeda, and L. Montero Mercadé, "A DUE based bilevel optimization approach for the estimation of time sliced OD matrices," in *Proc. Int. Symp. Transp. Simul. (ISTS) Int. Workshop Traffic Data Collection Standardisation (IWTDCS)*, 2014, pp. 1–19.

[9] X. Zhou and H. S. Mahmassani, "Dynamic origin-destination demand estimation using automatic vehicle identification data," *IEEE Trans. Intell. Transp. Syst.*, vol. 7, no. 1, pp. 105–114, Mar. 2006.

[10] S. Huang, A. W. Sadek, and L. Guo, "Computational-based approach to estimating travel demand in large-scale microscopic traffic simulation models," *J. Comput. Civil Eng.*, vol. 27, no. 1, pp. 78–86, Jan. 2013.

[11] C. Osorio, "Dynamic origin-destination matrix calibration for large-scale network simulators," *Transp. Res. C, Emerg. Technol.*, vol. 98, pp. 186–206, Jan. 2019.

[12] L. Shen, H. Shao, T. Wu, and W. H. K. Lam, "Spatial and temporal analyses for estimation of origin-destination demands by time of day over year," *IEEE Access*, vol. 7, pp. 47904–47917, 2019.

[13] K. N. Behara, A. Bhaskar, and E. Chung, "Novel approach for OD estimation based on observed turning proportions and Bluetooth structural information: Proof of the concept," in *Proc. Australas. Transp. Res. Forum (ATRF)*, Darwin, NSW, Australia, 2018, pp. 1–5.

[14] J. Ou, J. Lu, J. Xia, C. An, and Z. Lu, "Learn, assign, and search: Real-time estimation of dynamic origin-destination flows using machine learning algorithms," *IEEE Access*, vol. 7, pp. 26967–26983, 2019.

[15] K.-F. Chu, A. Y. S. Lam, and V. O. K. Li, "Deep multi-scale convolutional LSTM network for travel demand and origin-destination predictions," *IEEE Trans. Intell. Transp. Syst.*, early access, Jul. 10, 2019, doi: 10.1109/TITS.2019.2924971.

[16] E. Cipriani, M. Florian, M. Mahut, and M. Nigro, "A gradient approximation approach for adjusting temporal origin–destination matrices," *Transp. Res. C, Emerg. Technol.*, vol. 19, no. 2, pp. 270–282, 2011.

[17] H. Kim, S. Baek, and Y. Lim, "Origin-destination matrices estimated with a genetic algorithm from link traffic counts," *Transp. Res. Rec., J. Transp. Res. Board*, vol. 1771, no. 1, pp. 156–163, Jan. 2001.

[18] M. Florian and Y. Chen, "A coordinate descent method for the Bi-level O–D matrix adjustment problem," in *Int. Trans. Oper. Res.*, vol. 2, no. 2, pp. 165–179, 1995.

[19] J. T. Lundgren and A. Peterson, "A heuristic for the bilevel origin–destination-matrix estimation problem," *Transp. Res. B, Methodol.*, vol. 42, no. 4, pp. 339–354, 2008.

[20] D. Masip, T. Djukic, M. Breen, and J. Casas, "Efficient OD matrix estimation based on metamodel for nonlinear assignment function," presented at the Australas. Transp. Res. Forum, Darwin, NSW, Australia, 2018.

[21] C. Antoniou *et al.*, "Towards a generic benchmarking platform for origin–destination flows estimation/updating algorithms: Design, demonstration and validation," *Transp. Res. C, Emerg. Technol.*, vol. 66, pp. 79–98, May 2016.

[22] T. Djukic, S. Hoogendoorn, and H. Van Lint, "Reliability assessment of dynamic OD estimation methods based on structural similarity index," in *Proc. Transp. Res. Board 92nd Annu. Meeting*, Washington, DC, USA, 2013, p. 13, Paper 13-4851.
[23] K. N. S. Behara, A. Bhaskar, and E. Chung, "A novel approach for the structural comparison of origin-destination matrices: Levenshtein distance," *Transp. Res. C, Emerg. Technol.*, vol. 111, pp. 513–530, Feb. 2020.
[24] M. Bierlaire and P. L. Toint, "Meuse: An origin-destination matrix estimator that exploits structure," *Transp. Res. B, Methodol.*, vol. 29, no. 1, pp. 47–60, Feb. 1995.
[25] G. Cantelmo, F. Viti, C. M. J. Tampère, E. Cipriani, and M. Nigro, "Two-step approach for correction of seed matrix in dynamic demand estimation," *Transp. Res. Rec., J. Transp. Res. Board*, vol. 2466, no. 1, pp. 125–133, Jan. 2014.
[26] J. Doblas and F. G. Benitez, "An approach to estimating and updating origin–destination matrices based upon traffic counts preserving the prior structure of a survey matrix," *Transp. Res. B, Methodol.*, vol. 39, no. 7, pp. 565–591, 2005.
[27] B. Jaume and L. Montero, "An integrated computational framework for the estimation of dynamic OD trip matrices," in *Proc. IEEE 18th Int. Conf. Intell. Transp. Syst.*, Sep. 2015, pp. 612–619.
[28] J. Barcelö, L. Montero, L. Marqués, and C. Carmona, "Travel time forecasting and dynamic origin-destination estimation for freeways based on Bluetooth traffic monitoring," *Transp. Res. Rec., J. Transp. Res. Board*, vol. 2175, no. 1, pp. 19–27, Jan. 2010.
[29] H. Alibabai and H. S. Mahmassani, "Dynamic origin-destination demand estimation using turning movement counts," *Transp. Res. Rec., J. Transp. Res. Board*, vol. 2085, no. 1, pp. 39–48, Jan. 2008.
[30] C. Antoniou, M. Ben-Akiva, and H. N. Koutsopoulos, "Dynamic traffic demand prediction using conventional and emerging data sources," *Proc. Inst. Elect. Eng., Intell. Transp. Syst.*, vol. 153, no. 1, pp. 97–104, 2006.
[31] G. Michau *et al.*, "A primal-dual algorithm for link dependent origin destination matrix estimation," *IEEE Trans. Signal Inf. Process. Over Netw.*, vol. 3, no. 1, pp. 104–113, Mar. 2017.
[32] W. Mungthanya *et al.*, "Constructing time-dependent origin-destination matrices with adaptive zoning scheme and measuring their similarities with taxi trajectory data," *IEEE Access*, vol. 7, pp. 77723–77737, 2019.
[33] L. Liu, Z. Qiu, G. Li, Q. Wang, W. Ouyang, and L. Lin, "Contextualized spatial–temporal network for taxi origin-destination demand prediction," *IEEE Trans. Intell. Transp. Syst.*, vol. 20, no. 10, pp. 3875–3887, Oct. 2019.
[34] F. Calabrese, G. Di Lorenzo, L. Liu, and C. Ratti, "Estimating Origin-Destination flows using opportunistically collected mobile phone location data from one million users in Boston Metropolitan area," *IEEE Pervasive Comput.*, vol. 19, pp. 36–44, 2011.
[35] M. R. Nasab and Y. Shafahi, "Estimation of origin-destination matrices using link counts and partial path data," *Transportation*, pp. 1–28, 2019, doi: 10.1007/s11116-019-09999-1.
[36] X. Yang, Y. Lu, and W. Hao, "Origin-destination estimation using probe vehicle trajectory and link counts," *J. Adv. Transp.*, vol. 2017, pp. 1–18, 2017.
[37] M. S. Iqbal, C. F. Choudhury, P. Wang, and M. C. González, "Development of origin–destination matrices using mobile phone call data," *Transp. Res. C, Emerg. Technol.*, vol. 40, pp. 63–74, Mar. 2014.
[38] G. Michau, A. Nantes, A. Bhaskar, E. Chung, P. Abry, and P. Borgnat, "Bluetooth data in an urban context: Retrieving vehicle trajectories," *IEEE Trans. Intell. Transp. Syst.*, vol. 18, no. 9, pp. 2377–2386, Sep. 2017.
[39] M. Strickert, F.-M. Schleif, and U. Seiffert, "Gradients of pearson correlation for analysis of biomedical data," in *Proc. Argentine Symp. Artif. Intell. (ASAI)*, 2007, pp. 1–12.
[40] Aimsun, "Aimsun next 8.3 user's manual," in *Aimsun Next 8.3*. Barcelona, Spain: Aimsun, 2019.
[41] A. Bhaskar and E. Chung, "Fundamental understanding on the use of Bluetooth scanner as a complementary transport data," *Transp. Res. C, Emerg. Technol.*, vol. 37, pp. 42–72, Dec. 2013.
[42] A. Bhaskar, L. M. Kieu, M. Qu, A. Nantes, M. Miska, and E. Chung, "Is bus overrepresented in Bluetooth MAC scanner data? Is MAC-ID really unique?" *Int. J. Intell. Transp. Syst. Res.*, vol. 13, no. 2, pp. 119–130, May 2015.
[43] M. V. Chitturi, J. W. Shaw, J. R. Campbell IV, and D. A. Noyce, "Validation of origin–destination data from Bluetooth reidentification and aerial observation," *Transp. Res. Rec.*, vol. 2403, no. 1, pp. 116–123, 2014.
[44] *An Introduction to OpenStreetMap*, OpenStreetMap Found., London, U.K., 2014.
[45] *Australian Statistical Geography Standard (ASGS)*, Austral. Bureau Statist., Canberra, ACT, Australia, 2017.
[46] C. Osorio, "High-dimensional offline OD calibration for stochastic traffic simulators of large-scale urban networks," in *Technical Report*, ed. Cambridge, MA, USA: Massachusetts Institute of Technology, 2017.
[47] K. N. Behara, A. Bhaskar, and E. Chung, (2019). *Geographical window based structural similarity index for OD matrices comparison*. [Online]. Available: https://eprints.qut.edu.au/133466/[Working Paper]
[48] K. N. Behara, A. Bhaskar, and E. Chung, "Classification of typical Bluetooth OD matrices based on structural similarity of travel patterns: Case study on Brisbane city," in *Proc. Transp. Res. Board 97th Annu. Meeting*, Washington, DC, USA, 2018, p. 17, Paper 18-02285.
[49] S. Carrese, E. Cipriani, L. Mannini, and M. Nigro, "Dynamic demand estimation and prediction for traffic urban networks adopting new data sources," *Transp. Res. C, Emerg. Technol.*, vol. 81, pp. 83–98, Aug. 2017.
[50] M. Nigro, E. Cipriani, and A. del Giudice, "Exploiting floating car data for time-dependent origin–destination matrices estimation," *J. Intell. Transp. Syst.*, vol. 22, no. 2, pp. 159–174, 2018.

Krishna N. S. Behara received the bachelor's degree (Hons.) in civil engineering and the master's degree in transportation engineering from the Birla Institute of Technology and Science (BITS)-Pilani, India, and the Ph.D. degree from the Queensland University of Technology (QUT), Brisbane, QLD, Australia. He is currently a Post-Doctoral Research Fellow with QUT. His research interests include traffic modeling and simulation, transport data analytics, and travel behavior modeling.

Ashish Bhaskar received the bachelor's degree in civil engineering from IIT Kanpur, Kanpur, India, the master's degree from The University of Tokyo, Tokyo, Japan, and the Ph.D. degree from the Swiss Federal Institute of Technology (EPFL), Lausanne. He is currently an Associate Professor with QUT. His research interests include transport data analytics, transport modeling and simulation, and traffic management and control.

Edward Chung received the B.Eng. (Hons.) and Ph.D. degrees from Monash University, Australia. He is currently a Professor with The Hong Kong Polytechnic University and an Adjunct Professor with the Queensland University of Technology. His research interests include traffic management, machine learning, and transport modeling.